Pellet Injector for Diagnostics Purposes

P.T. Lang, P. Cierpka, S.M. Egorov*, T. Kass,
B.V. Kuteev*, P.V. Reznichenko*, V.Yu. Sergeev*,
H. Vetter, G. Weber

IPP 1/280

July 1994

MAX-PLANCK-INSTITUT FÜR PLASMAPHYSIK

85748 GARCHING BEI MÜNCHEN

MAX-PLANCK-INSTITUT FÜR PLASMAPHYSIK

GARCHING BEI MÜNCHEN

Pellet Injector for Diagnostics Purposes

P.T. Lang, P. Cierpka, S.M. Egorov*, T. Kass,
B.V. Kuteev*, P.V. Reznichenko*, V.Yu. Sergeev*,
H. Vetter, G. Weber

IPP 1/280 July 1994

*State Technical University of St. Petersburg
Polytechnicheskaya 29, St. Petersburg, Russia 195251

Die nachstehende Arbeit wurde im Rahmen des Vertrages zwischen dem Max-Planck-Institut für Plasmaphysik und der Europäischen Atomgemeinschaft über die Zusammenarbeit auf dem Gebiete der Plasmaphysik durchgeführt.

PELLET INJECTOR FOR DIAGNOSTICS PURPOSES

P.T. Lang, P. Cierpka, S.M. Egorov*, T. Kass, B.V. Kuteev*,
P.V. Reznichenko*, V.Yu. Sergeev*, H. Vetter, and G. Weber

Max-Planck-Institut für Plasmaphysik
EURATOM Association
85748 Garching bei München, Germany
*State Technical University of St. Petersburg
Polytechnicheskaya 29
St. Petersburg, Russia 195251

ABSTRACT

We report the design, construction and the testbed results for a novel compact gas gun injector for solid diagnostic pellets of different sizes and materials. The injector was optimized for the diagnostic requirements of the ASDEX Upgrade tokamak, yielding the possibility of a widely varying deposition profile of ablated material inside the plasma. This allows variation of the pellet velocity and the total number of injected atoms. The use of different propellant gases (He, N_2, H_2) results in an accessible velocity range from about 150 m/s to more than 600 m/s in the case of spherical carbon pellets with masses ranging from 2×10^{18} to 10^{20} atoms. Both the scattering angle (~1°) and the maximum propellant gas throughput to the tokamak (less than 10^{16} gas particles) were found to be sufficiently low. The injector provided both high efficiency ($\geq$ 85%) and high reliability during the whole testbed operation period and also during the first injection experiments performed on ASDEX Upgrade. The pellet velocities achieved for different propellant gas pressures, pellet diameters, and pellet materials were analyzed. We found that, although the pellet diameters range from 0.45 to 0.85 times the barrel diameter, the pellet acceleration is mostly caused by gas drag. Pellet velocities in excess of those calculated on the basis of the gas drag model were observed. Additional acceleration that increases with the pellet diameter contrary to the gas drag model may be explained by the influence of the pellet on the gas dynamics in the barrel.

Table of Contents

1. INTRODUCTION

During the last few decades, high-speed techniques for accelerating macroscopic particles (pellets) have been greatly boosted by the requirements of fusion-oriented plasma physics. Conversely, fusion-oriented plasma physics has derived many benefits from the development of high-speed pellet acceleration techniques. One of the main improvements is the (re)fuelling of the hot confined plasma by injecting frozen, mm-sized hydrogen pellets. Another application of pellet injection technique in fusion research is to diagnose the plasma with a probe particle. Such diagnostic pellets, often produced from carbon, have been used for measuring the plasma electron temperature [1], the effective charge [2] and the transport coefficients of both the bulk plasma [3] and the impurities [4]. Diagnostics of the magnetic field configuraton [5, 6], plasma current density [7] and alpha particles [8] are now being developed by means of pellet injection.

Up to now, many different devices for pellet acceleration have been developed. Most of them enlist one of the two basic concepts: centrifuge and gas gun. A centrifuge injector is a mechanical device that uses centrifugal forces to accelerate pellets constrained to move in a track or groove on a high-speed rotating disk, arbor or arm. Centrifuge accelerators are most commonly used for refuelling with hydrogen up to medium velocities (~1.2 km/s [9]) since the mechanical stability of the disk, arbor or arm restricts the acceleration potential. The simplest and most frequently employed pellet acceleration technique, however, is the gas gun, which operates on a pneumatic principle in which compressed gas provides the driving force. Kinetic energy is transferred to the pellet inside the barrel from the internal energy of the gas. Since the ultimate velocities achievable with a simple one-stage light gas gun are limited, more sophisticated constructions such as gas guns operating with hot propellant gas and two- or three-stage gas guns were developed. In this way, velocities of more than 10 km/s were obtained [10].

Nearly every pellet injector is designed and constructed to meet a special requirement. There are injection systems specialized to achieve very high velocities or very large pellet masses. Others are optimized to allow a very high repetition rate in order to make density control of the plasma possible by adjusting the pellet injection frequency. In this paper we report the design, construction and testing of a compact, easily handled single-stage gas gun injector for room temperature solid pellets of different sizes and materials. As our injector offers the possibility of changing both the pellet velocity and the pellet mass, a widely varying deposition profile of the pellet material inside the plasma can be obtained. This allows very close adaption to the requirements of a specific experimental investigation.

2. GAS GUN INJECTION SYSTEM

The objective was to develop a system for injecting diagnostic pellets into the ASDEX Upgrade tokamak, that is easy to handle and fully automatic. As there is usually no access to the equipment between plasma discharges, the injector had to be equipped with a pellet charger unit. The injector was designed to achieve features optimized to meet plasma diagnostic requirements. Calculations based on the neutral gas shielding model [1] showed that a carbon pellet 0.7 mm in diameter, accelerated to about 600 m/s, can reach the plasma centre in ASDEX Upgrade. To allow the widest possible variation of the ablated pellet particle deposition profile inside the plasma, it was necessary to vary the pellet mass in addition to the pellet velocity. For this purpose, a system able to handle different pellet diameters was designed. The intention to use the injector as a diagnostic tool in a fusion experiment made minimization of the propellant gas puffing into the fusion device a major concern of the design and construction. In order to facilitate localization of the ablated pellet material inside the plasma and improve the diagnostic scope, minimum angular scattering of the pellets leaving the injector was a design objective.

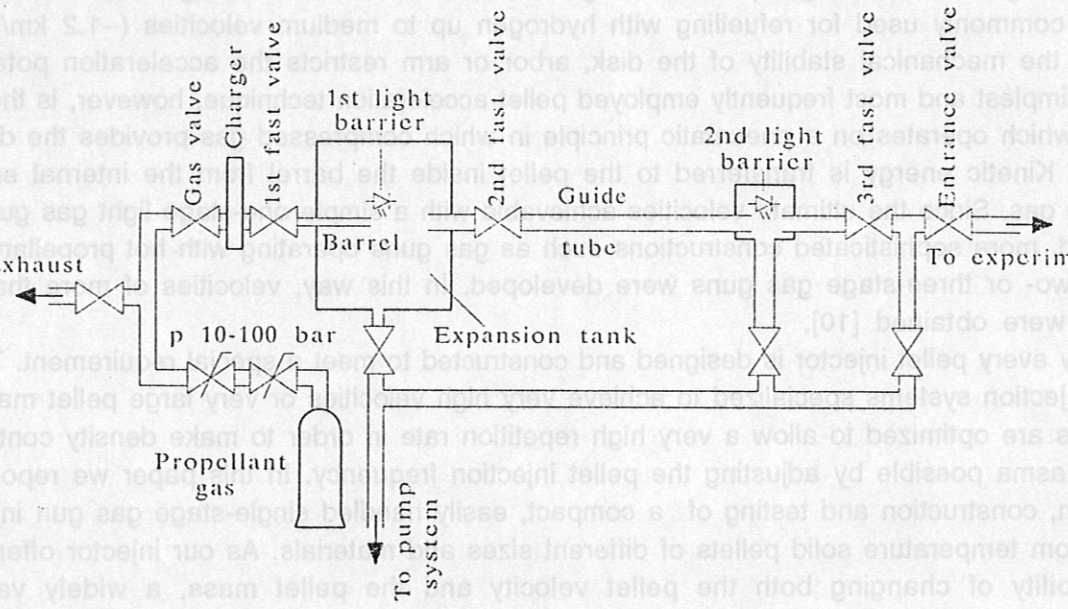

Fig. 1: *Schematic drawing of the experimental setup.*

A sketch of the experimental arrangement finally used for our pellet injector is shown in Fig. 1. The propellant gas supply system allows the gas pressure to be adjusted up to 100 bar; for some shots in the testbed a gas bottle containing He at 150 bar was also directly connected to the gas pipes. Up to 90 pellets with diameters from 0.2 to 0.7 mm can be stored within the rotated magazine of the pellet gun charger; an electric motor rotates the charging disk automatically to the next position after each pellet shot. A fast propellant gas valve and three fast electromagnetic valves are installed along the pellet path. The propellant gas valve and the first fast valve control the acceleration process inside the 120 mm long stainless-steel gun barrel with a diameter of 0.85 mm. The second and third fast valves, together with the guide tube and the expansion tank, are used to decrease the amount of propellant gas

escaping from the injector into the tokamak. A pumping system (a turbomolecular pump with backing forepump) is used to evacuate the whole pellet travel line to a pressure below 10^{-5} Pa before a shot and prevents a strong pressure increase near the injector exit. All opening and closing times of fast valves 2 and 3 can be adjusted electronically. Light barrier arrangements are installed along the pellet path to provide a time-of-flight measurement of the pellet velocity. The pellet is guided to the entrance of the tokamak or the test facility by a 2.05 m long stainless-steel tube with a diameter of 5 mm, mounted inside a carrier tube. The injector system is separated from the fusion device by a pneumatic entrance valve and an electrical isolating adapter.

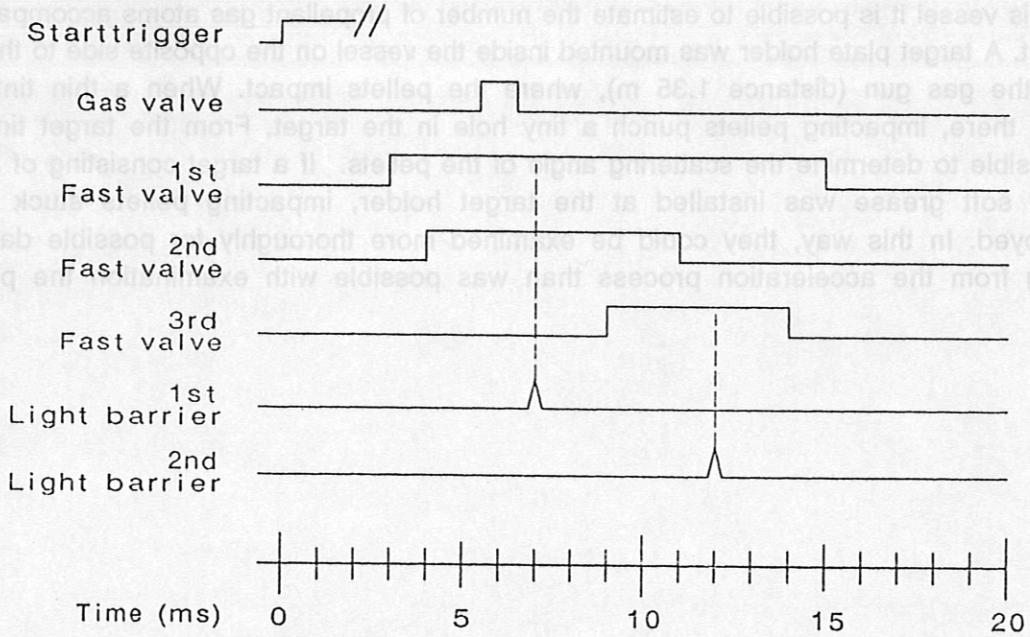

Fig. 2 : *Schematic diagram of a pellet shot sequence*

A diagram of a typical pellet shot sequence is given in Fig. 2, where the timing of the opening periods for the different valves are displayed. If a pellet request trigger is received by the control electronics, the first fast valve is opened to initiate acceleration. Thereby, the pellet is accelerated to a few m/s by the small amount of air contained in the charger. Then, approximately 0.5 ms later, the accelerating high-pressure propellant gas pulse is applied to the pellet by opening the gas valve. Fast valves 2 and 3 open for a short period (~5 ms) to allow passage of the pellet, but block most of the streaming propellant gas.

The injector system (including the vacuum system) and the data acquisition are operated fully automatically by a computer system consisting of a Siemens Simatic S5 programmable logic controller and a COROS work station. This is responsible for pumping down the system after a shot, initiating and controlling the charging and finally controls the main shot sequence. A pellet request trigger is received - provided the permission signal is valid - from the ASDEX Upgrade local timer system, delayed by a desired period with respect to the moment of plasma initiation. To prevent damage to the fusion device by pellets, an inhibit is included for plasma densities or currents in the tokamak that are too low for pellet injection.

While the injector was being operated on the testbed, a few additional diagnostic features were applied. First, a photo station was mounted at the exit of the injector to take a picture of the pellet in flight. To avoid movement blur caused by the high velocity of the pellet, a short infrared laser pulse emitted from a GaAs laser diode (wavelength 904 nm, pulse duration 70 ns FWHM) was applied for illumination. Observation was performed by an infrared-sensitive CCD camera, the current picture being captured by an electronic freezer and then documented on videotape. These pictures not only allow a check of whether the pellet is subject to deformation or even destruction; as the time the laser fires is also well known, an additional velocity measurement is made. After crossing the photo station the pellet enters a target vessel pumped down to about 10^{-5} Pa. From the time development of the pressure inside this vessel it is possible to estimate the number of propellant gas atoms accompanying the pellet. A target plate holder was mounted inside the vessel on the opposite side to the exit port of the gas gun (distance 1.35 m), where the pellets impact. When a thin tinfoil is installed there, impacting pellets punch a tiny hole in the target. From the target tinfoil it was possible to determine the scattering angle of the pellets. If a target consisting of a thin layer of soft grease was installed at the target holder, impacting pellets stuck there undestroyed. In this way, they could be examined more thoroughly for possible damage resulting from the acceleration process than was possible with examination the picture alone.

3. EXPERIMENTAL RESULTS

The pellets used for the investigations described here were either perfect spheres made of carbon or silicon cubes. For our experiments, carbon pellets of preselected diameters were sorted into different species, each consisting of only pellets with diameters differing by less than 50 µm. Six of these species with diameters 400, 450, 500, 550, 600 and 650 µm were used for the measurements presented. The values given for the pellet diameters always refer to the lowest diameter of the species used, e.g. d = 600 µm means pellets with diameters ranging from 600 to 650µm. All the silicon pellets used had side lengths of 600 µm.

3.1 Optimization of the shot sequence

In testbed operation, first the optimum time sequence for opening and closing the gas valve and fast valves was worked out. Therefore, two requirements had to be satisfied simultaneously: the pellets had to pass through all the valves without any obstruction and the gas puff to the test vessel had to be minimized. Whereas for the first condition a long opening period is advantageous, the latter calls for minimization of the opening. As a first attempt, two identical expansion tanks with the three fast valves were just mounted in series behind the gun barrel. Thus, the pellet passed through all valves before entering the guiding tube. However, no satisfactory operation sequence was found in this way. For opening sequences allowing highly reliable operation, a gas puff of the order of 10^{18} propellant gas particles was required. Drastically improved performance was achieved with the configuration shown in Fig. 1: the expansion tank (V = 5 liter) and the second fast valve were mounted just behind the gun barrel, the third fast valve behind the guide tube. This arrangement provides an additional advantage since it reduces space requirements near the entrance port of the tokamak. Gas throughput of less than $5 * 10^{15}$ particles to the tokamak with an applied propellant gas pressure of 100 bar was achieved when the expansion tank was disconnected by closing the pump valve just before the shot while still pumping near the injector exit. This status has to be maintained for a few seconds until the entrance valve to the test vessel is closed again (simulating the opening time of the entrance valve to the tokamak during a plasma discharge); evacuation of the expansion tank occurred after the shot sequence during preparation for the next shot. With this mode of operation, the opening times of the fast valves were found to be not very critical. Even with the valves kept open for a few tens of milliseconds - a time more than sufficient for reliable operation at all velocities achieved - there was no troublesome increase of gas throughput. The only critical sequence remaining for reliable injection was found to be the opening of the propellant gas valve and the first valve; optimum results were obtained by opening the gas valve from 0.5 to 1 ms, delayed with respect to the opening of the first fast valve. If delay times are too short, the pellets are damaged whereas with longer delay times there is a strong increase in shot-to-shot velocity fluctuations.

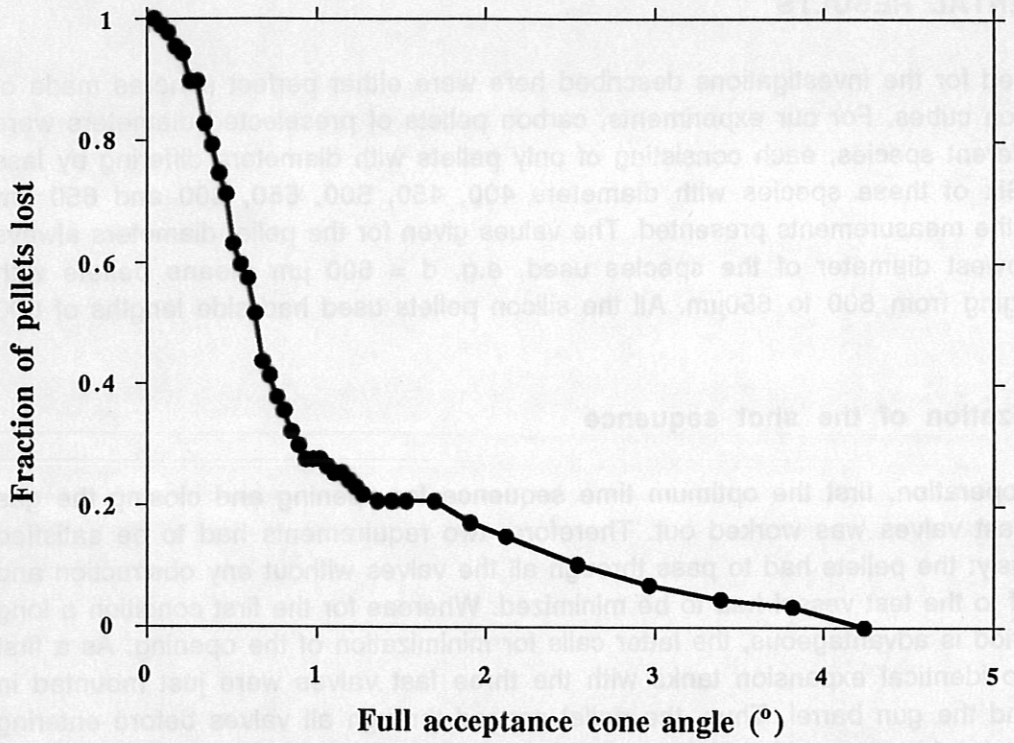

Fig. 3: *Fraction of pellets missed at a fixed cone angle. Data covering target foils for all the different pellet diameters, comprising data from more than 300 pellet shots.*

3.2. Stray angle and pellet integrity

Angular pellet scattering, as observed by analysing the tinfoil target, was found to show no noticeable dependence on the pellet velocity or diameter. In our final setup, the guiding tube was centred inside a carrier tube by sets of adjustable needles and finally fixed by a residual tensile force. The different parts were carefully aligned by means of a laser beam as a guiding line. By performing the installation in this way more than 70% of all pellets passing through both light barriers arrived undestroyed within a cone angle of 1 degree. In Fig. 3 an analysis of the target foils is presented, giving the fraction of pellets missing within a specified cone angle. For each pellet diameter a separate target was analysed, but as they show no noticeable difference all data were used for this plot. As can be clearly seen from the data, there is a large fraction of pellets having a small angular distribution of about one degree on which a smaller fraction of pellets having a much wider angular spread is superimposed. The former are undamaged pellets, whereas the latter could be clearly identified as damaged pellets. From the impact traces on the tinfoil, the photographic diagnostics and the grease impact it was found that target-damaged pellets consisted of no more than two or three big parts and a small fraction of carbon dust. Thus, even if a pellet is damaged during the acceleration process, it can still be used for plasma diagnostics. Reliable differentiation between damaged and undamaged pellets was afforded by the two light barrier signals since the cloud of carbon dust resulting from damage causes a long tail in the slope of the photodiode voltage. Light barrier signals recorded for

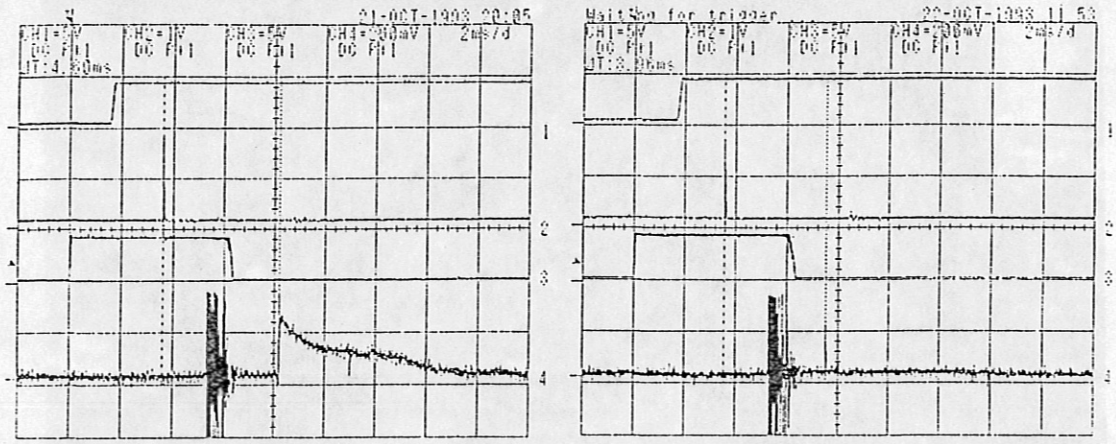

Fig. 4: *Channel 4 showing light barrier signals recorded for an undamaged pellet (right) and a pellet damaged before passing the second light barrier(left); channel 2: first light barrier, channels 1 and 3: 1st and 2nd fast valves.*

an undamaged pellet and a pellet damaged before passing the second light barrier are shown for comparison in Figure 4.

Figure 5 shows a photograph taken through a microscope showing four carbon pellets with diameters from 400 to 700 µm. These pellets were injected into the grease target with He as propellant gas at the maximum nominal operation pressure of 100 bar. All these pellets (and also a few tens of more pellets examined after being accelerated) show no noticeable damage. Without any abnormal indication from the photodiode signal, pellets can thus be assumed to have retained their perfectly spherical shape without any substantial loss of mass after acceleration - an important fact for the analysis and modelling of the pellet evaporation process inside the plasma.

For the test shots and all the measurements reported in this paper, our gas gun was fired more than two thousand times in the testbed. Successful pellet acceleration was observed in about 85% of these shots, while 10% resulted in the ejection of a (slightly) damaged pellet. Once the testbed programme was completed, the injector was finally mounted onto ASDEX Upgrade, where a few hundred further test shots and also a couple of injection shots into the plasma were performed. During this whole period, both in the testbed and on the tokamak, our injector showed reliable performance.

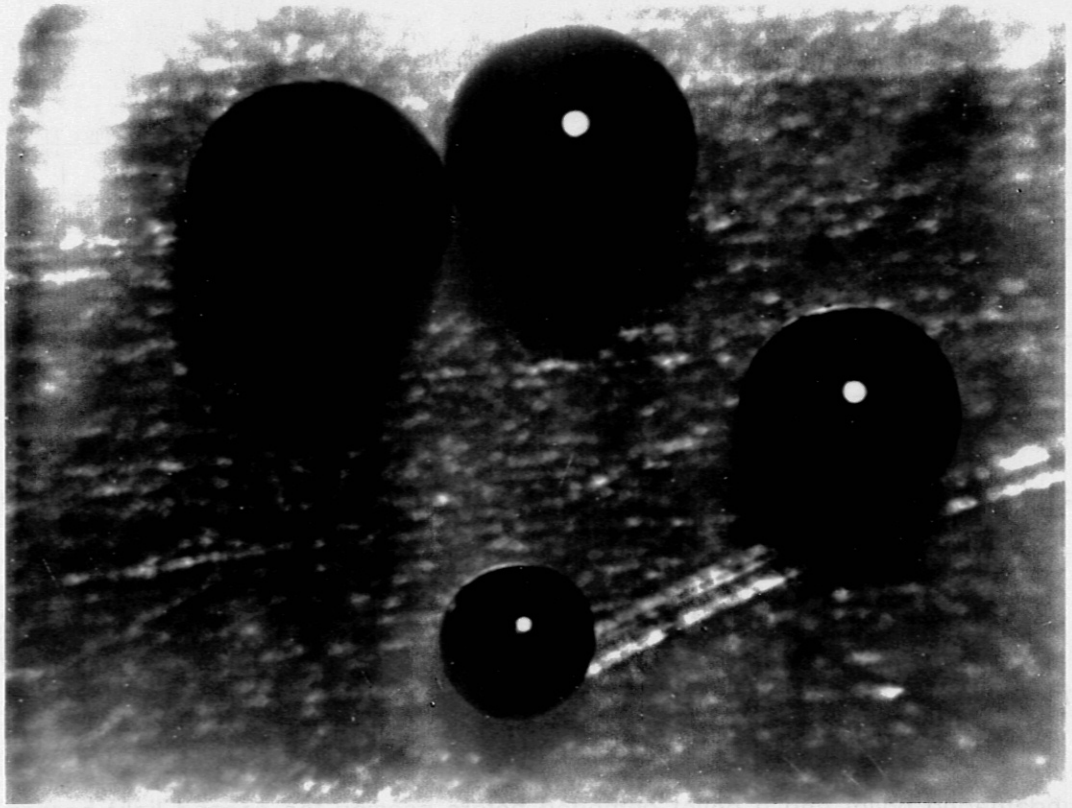

Fig. 5: *Carbon pellets with diameters from 400 to 700 μm after injection into a grease target by means of He propellant gas at 100 bar. Photography taken through a microscope after extraction from the target.*

3.3. Variation of pellet mass

Pellet velocities measured under optimized shot conditions versus the propellant gas pressure are shown in Fig. 6. For these measurements helium was used as propellant gas to accelerate pellets 600 μm in diameter. An increase in pellet velocity can be observed when the propellant gas pressure is increased to 100 bar, but saturation of the pellet muzzle velocity occurs at higher pressures. If a pressure of 150 bar is applied, no significant further increase in pellet velocity is detected. Thus, the maximum pressure for standard injector operation allows acceleration to a velocity of about 600 m/s, which seems to be the limit of the device in its present form. At a fixed propellant gas pressure velocity variations of about ±10% were observed; the same value was also found for other pellet diameters or propellant gases. The solid line in Fig. 6 is obtained from a least square fit to the experimental data. The curves given in Fig. 7 are obtained in the same way, representing the measured pellet velocities obtained for different pellet diameters with helium as propellant gas. As can be seen from the plot, smaller pellet velocities are achieved at a given pressure for reduced diameters of the carbon spheres, whereas the general behaviour of the velocity with pressure is nearly unaffected. A closer look at this behaviour with respect to different theoretical models of the acceleration process is given in the next section.

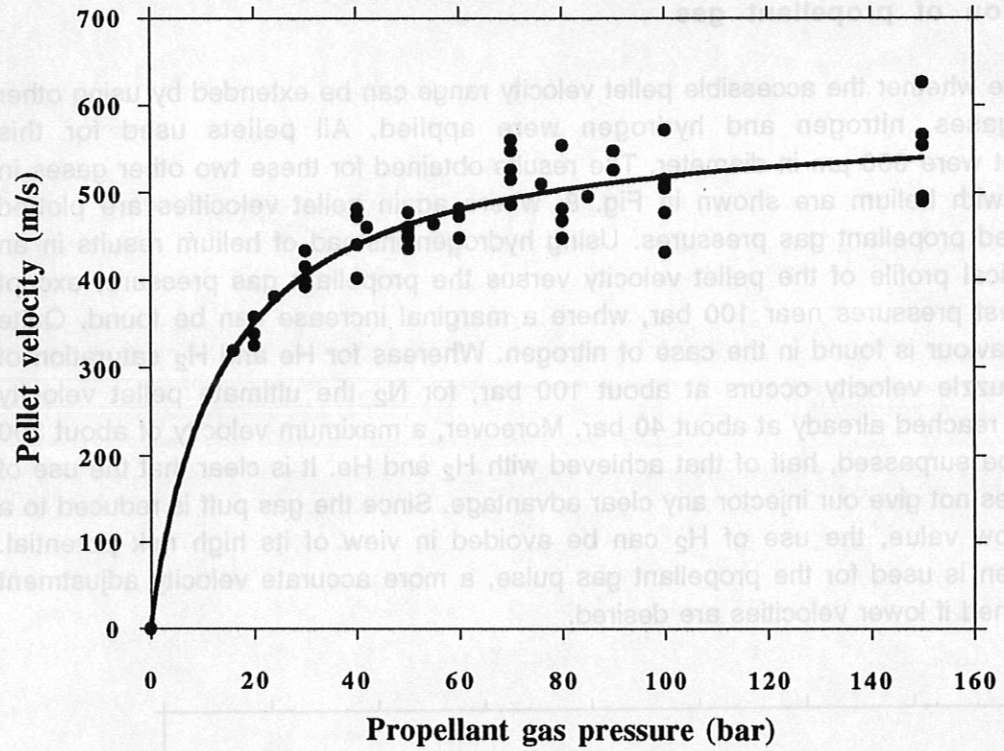

Fig. 6: *Pellet velocities versus applied helium propellant gas pressure (filled dots) for carbon pellets 600 μm in diameter; the solid line is a least square fit to the data.*

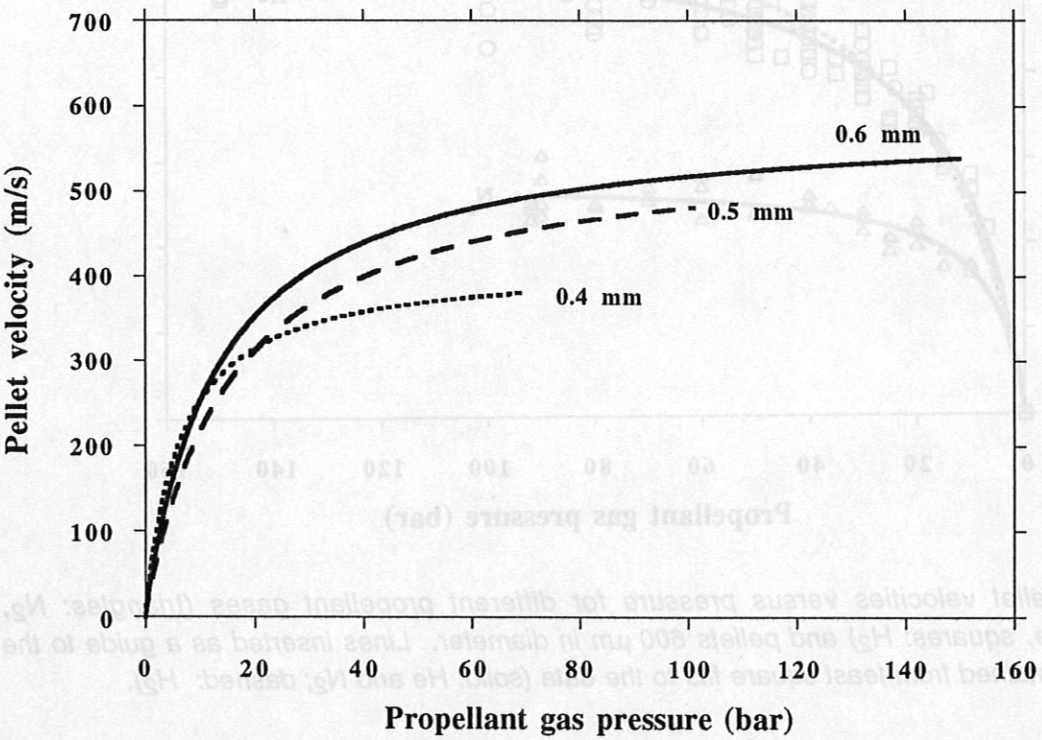

Fig. 7: *Least square fits to the pellet velocities measured for pellets of different diameters.*

3.4. Variation of propellant gas

To investigate whether the accessible pellet velocity range can be extended by using other propellant gases, nitrogen and hydrogen were applied. All pellets used for this measurement were 600 μm in diameter. The results obtained for these two other gases in comparison with helium are shown in Fig. 8, where again pellet velocities are plotted versus applied propellant gas pressures. Using hydrogen instead of helium results in an almost identical profile of the pellet velocity versus the propellant gas pressure, except for the highest pressures near 100 bar, where a marginal increase can be found. Quite different behaviour is found in the case of nitrogen. Whereas for He and H_2 saturation of the pellet muzzle velocity occurs at about 100 bar, for N_2 the ultimate pellet velocity seems to be reached already at about 40 bar. Moreover, a maximum velocity of about 300 m/s cannot be surpassed, half of that achieved with H_2 and He. It is clear that the use of hydrogen does not give our injector any clear advantage. Since the gas puff is reduced to a sufficiently low value, the use of H_2 can be avoided in view of its high risk potential. When nitrogen is used for the propellant gas pulse, a more accurate velocity adjustment can be obtained if lower velocities are desired.

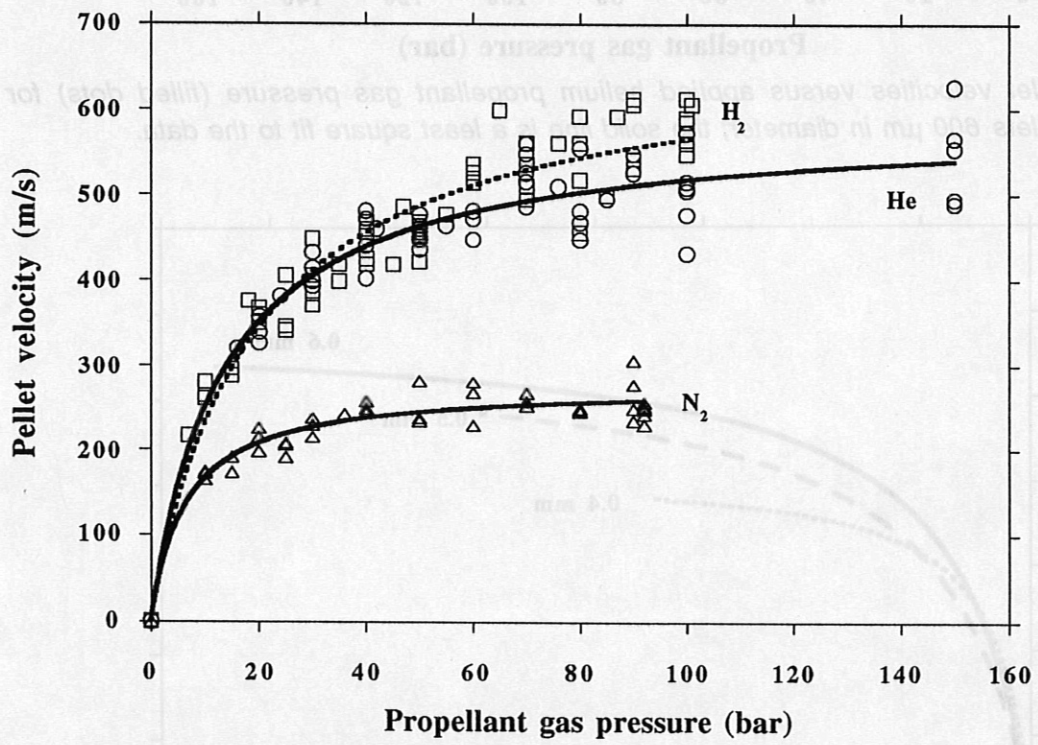

Fig. 8: *Pellet velocities versus pressure for different propellant gases (triangles: N_2, circles: He, squares: H_2) and pellets 600 μm in diameter. Lines inserted as a guide to the eye are obtained from least square fits to the data (solid: He and N_2; dashed: H_2).*

3.5. Variation of pellet material

To prove the ability of the injection system for accelerating different types of pellets, some test shots using cubic silicon pellets were performed. Here, only a single species of cubic silicon pellets with side length of 600 μm were used. As propellant gas helium was applied. The velocities measured are plotted with respect to the propellant gas pressure in Fig.9; for comparison pellet velocities achieved for carbon pellets of almost similar size are also plotted. Due to the higher mass density, for a given acceleration configuration velocities are smaller for the silicon pellets. However, also for such pellets velocities of several hundred m/s can be achieved easily. Some trouble occured from the cubic shape of the silicon pellets; when rotating the charger disk filled with silicon pellets the cubes sometimes hooked on the brass drum causing damage of the electric motor for disk rotation. Therefore, only spherical pellets should be used to guarantee maximum reliable operation of the injector.

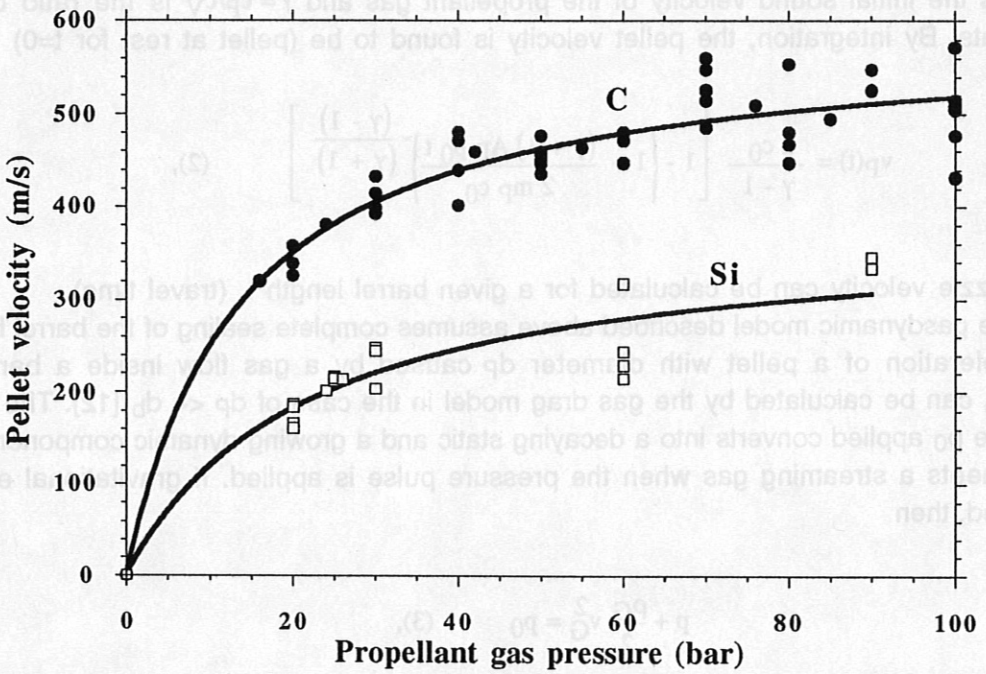

Fig. 9: *Pellet velocities versus applied helium propellant gas pressure for spherical carbon pellets 600 μm in diameter (filled dots) and for cubic silicon pellets (open squares) with side length 600 μm; the solid lines are least square fits to the data.*

4. COMPARISON OF MEASURED PELLET VELOCITIES WITH DIFFERENT ACCELERATION MODELS

The performance of most single-stage gas guns reported [11] was found to be properly modelled (with a consistent decrease from ideal performance by about 15%) by an analytic theory based on the similarity principle. This theory assumes nonsteady, isentropic, one-dimensional gas flow in an infinite barrel of constant radius; the motion of the pellet is then governed by the propagation of simple rarefraction waves into the high-pressure medium. The acceleration of a pellet with mass m_P and cross-section A_P to a velocity v_P by applying a pressure p_0 to one side of the pellet while the projectile moves into the vacuum is governed in the absence of nonideal effects by the equation of motion:

$$m_P \frac{dv_P}{dt} = p_0 A_P \left\{1 - \left(\frac{1}{2}\frac{(\gamma - 1) v_P}{c_0}\right)\right\}^{\frac{2\gamma}{\gamma-1}} \qquad (1),$$

where c_0 is the initial sound velocity of the propellant gas and $\gamma = c_P/c_V$ is the ratio of the specific heats. By integration, the pellet velocity is found to be (pellet at rest for t=0)

$$v_P(t) = \frac{2 c_0}{\gamma - 1}\left[1 - \left\{1 + \frac{(\gamma + 1) A_P p_0 t}{2 m_P c_0}\right\}^{-\frac{(\gamma - 1)}{(\gamma + 1)}}\right] \qquad (2),$$

and the muzzle velocity can be calculated for a given barrel length L (travel time).
Whereas the gasdynamic model described above assumes complete sealing of the barrel by the pellet, acceleration of a pellet with diameter d_P caused by a gas flow inside a barrel of diameter d_b can be calculated by the gas drag model in the case of $d_P << d_b$ [12]. The initial gas pressure p_0 applied converts into a decaying static and a growing dynamic component, i.e. the pellet meets a streaming gas when the pressure pulse is applied. If gravitational effects are neglected, then

$$p + \frac{\rho_G}{2} v_G^2 = p_0 \qquad (3),$$

where ρ_G and v_G are the local propellant gas density and velocity, respectively. Assuming that it is only the dynamic pressure acting on the pellet that transfers a fraction of energy given by the geometrical drag coefficient c_W, the equation of motion in the laboratory reads

$$m_P \frac{dv_P}{dt} = A_P c_W \frac{\rho_G(x)}{2} (v_G(x) - v_P(x))^2 \qquad (4).$$

To solve equation (4), the distributions of both the gas density and velocity along the barrel axis are required. As for the operation parameters of our injector the Reynold's numbers ranged from Re $=10^3$ to 10^5; the gas flow can be assumed to be turbulent. Therefore, we

apply a model [13] considering turbulent gas flow and including friction at the wall surface. According to this model, the gas velocity distribution along the barrel is described by

$$\left(\frac{v_c}{v_G(0)}\right)^2 - \left(\frac{v_c}{v_G(x)}\right)^2 - 2\ln\frac{v_c}{v_G(x)} = \frac{2\gamma}{\gamma+1}\xi\frac{x}{d_b} \qquad (5).$$

A best fit to the experimental data is obtained in [13] for a friction coefficient $\xi = 0.3164/Re^{1/4}$; the critical velocity $v_c = c_0\sqrt{2/(\gamma+1)}$ is the ultimate gas velocity at the exit of the tube. The gas density distribution required to solve equation (4) can be obtained from the continuity equation,

$$\rho_G(x) = \rho_G(0)\frac{v_G(0)}{v_G(x)} \qquad (6),$$

where $\rho_G(0)$ is determined by the applied propellant gas pressure p_0. The set of equations (4) to (6) allows the pellet muzzle velocity v_P to be calculated for a given gas pressure p_0.

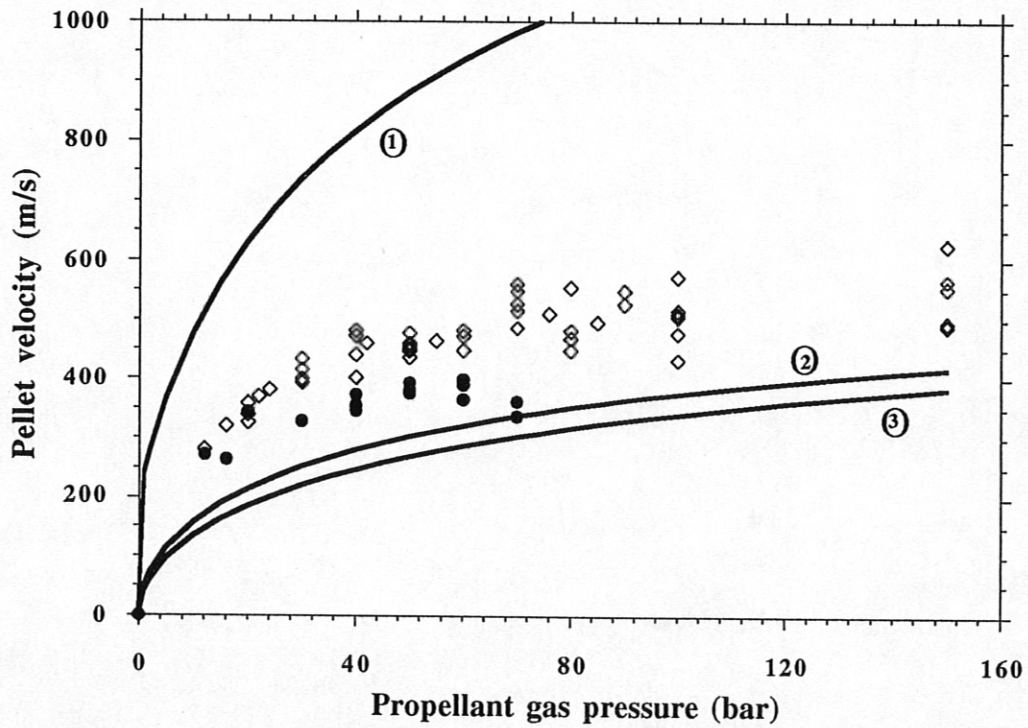

Fig. 10: *Comparison of measured pellet muzzle velocities $v_P = v_P(p_0)$ (filled dots: d_P = 400 µm; open squares: d_P = 600 µm) and those calculated with the pellet acceleration models. Curve 1 is evaluated with the gas expansion model for $d_P = d_b$ = 800 µm. Curves 2 (d_P = 400 µm) and 3 (d_P = 600 µm) are obtained by means of the gas drag model.*

The measured pellet muzzle velocities versus applied gas pressures p_0 and those calculated with both pellet acceleration models are shown in Fig. 7. It can be seen that for a pellet diameter of 400 µm measured velocities slightly (by up to 30%) exceed those obtained with the gas drag model (curve 2). As can be found by comparing the calculated curves 2 (d_P = 400 µm) and 3 (d_P = 600 µm), the gas drag model predicts a decreasing pellet velocity for increasing pellet diameter, because the pellet acceleration is proportional to the area density A_P/m_P (see equation 3). Experimental velocity values for d_P = 600 µm sized pellets exceed the predictions of the gas drag model by a factor of up to about 2. This behaviour can presumably be explained by the influence of pellets on the gas flow process since the pellet size becomes comparable with the barrel diameter d_b = 850 µm. In fact, for the case with d_P = 600 µm, pellet velocities should probably be in the vicinity of curve 1 in Fig. 10. This curve was calculated by the ideal gas expansion model assuming $d_P = d_b$ = 800 µm. Therefore, it is concluded that the experimental conditions for accelerating sufficiently large pellets is at the transition between the two pellet acceleration models presented above.

5. INTEGRATION INTO THE ASDEX UPGRADE SETUP

The diagnostic injector is mounted at ASDEX Upgrade in sector 5 above the pellet centrifuge. A radial section of the setup at the torus is given in Fig. 11. Like the trajectory of the cryogenic fuelling pellets of the centrifuge, the injection path of the diagnostic pellets is tilted by 11° from the radial direction towards sector 4. In order to enable observation of the diagnostic pellets via the same optical setups as used for instrumentation observing cryogenic pellet ablation, both injection path had to be close together. Therefore, diagnostic pellets are injected with a tilt angle of 5.5° with respect to the horizontal plane, crossing the level of cryogenic pellet injection (75 mm above the torus midplane) at R = 2.00 m.
To prohibit pellet injection at unsuitable plasma conditions, the injectors local control unit is connected to the AUG safety and interlock system. The system is also equipped with a local timer to adjust pellet injection with respect to the start of a plasma discharge (TS06 trigger signal). Furthermore, initiation of the injection sequence upon a request signal arriving from the fast control unit (SSR) is also possible.

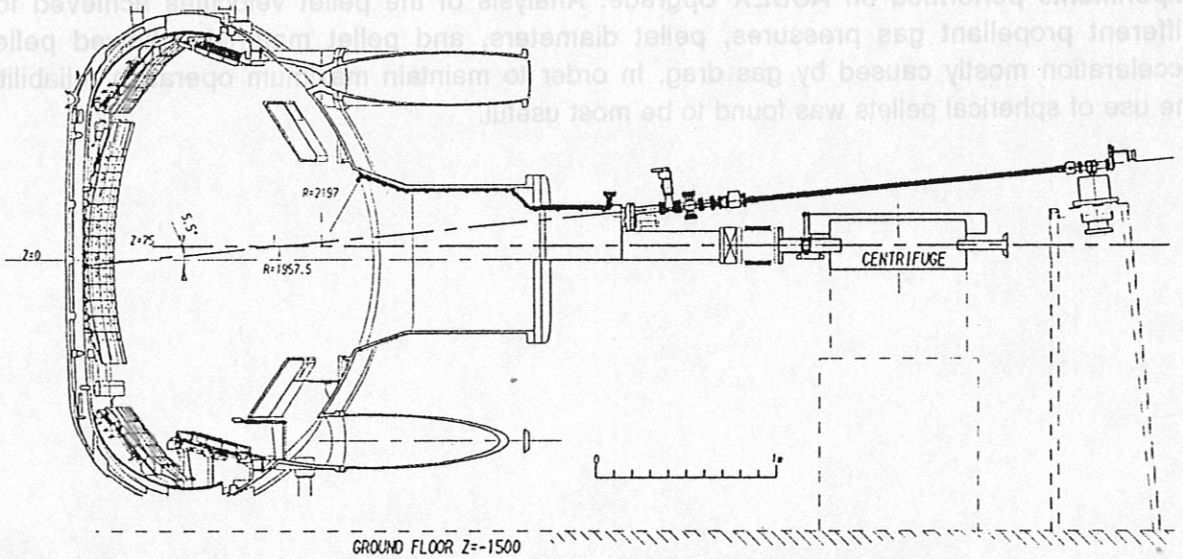

Fig. 11: *Radial section of the ASDEX Upgrade vessel with diagnostic pellet injector adapted.*

6. SUMMARY

The novel compact gas gun injector for single solid diagnostic pellets of different sizes and materials described here has been successfully tested and has proved to operate well and reliable both in the testbed and at the torus. With this system, optimized for the diagnostic requirements of the ASDEX Upgrade tokamak, the possibility of a widely varying deposition profile of ablated material inside the plasma is yielded by variation of the pellet velocity and the total number of injected atoms. The use of different propellant gases (He, N_2, H_2) results in an accessible velocity range from about 150 m/s to more than 600 m/s in the case of spherical carbon pellets with masses ranging from 2 x 10^{18} to 10^{20} atoms. For cubic silicon pellets, velocities up to 350 m/s can be obtained. Both the scattering angle (~1°) and the maximum propellant gas throughput to the tokamak (less than 10^{16} gas particles) were found to be sufficiently low. The injector provided both high efficiency ($\geq$ 85%) and high reliability during the whole testbed operation period and also during the first injection experiments performed on ASDEX Upgrade. Analysis of the pellet velocities achieved for different propellant gas pressures, pellet diameters, and pellet materials showed pellet acceleration mostly caused by gas drag. In order to maintain maximum operation reliability the use of spherical pellets was found to be most useful.

REFERENCES

[1] N.L. Vasin, S.M. Egorov, Yu.V. Esipchuk, B.V. Kuteev, and V.Yu. Sergeev, Sov. J. Plasma Phys. **12**, 73 (1986).

[2] N.L. Vasin, N.M. Gegechkori, S.M. Egorov, V.A. Krupin, B.V. Kuteev, A.B Pimenov, and V.Yu. Sergeev, Sov. J. Plasma Phys. **10**, 650 (1984).

[3] A.A. Bagdasarov, S.M. Egorov, B.V. Kuteev, V.A. Rozhanskii, and V.Yu. Sergeev, Sov. J. Plasma Phys. **12**, 449 (1987).

[4] T-10 Group, in *Proceedings of the 10th International Conference on Plasma Physics and Controlled Nuclear Fusion Research 1984* , London, 1984 (International Atomic Energy Agency, Vienna, 1985), Vol. 1, pp. 181-192.

[5] S.M. Egorov, B.V. Kuteev, I.V. Miroshnikov, V.Yu. Sergeev, Sov. J. Pizma v JETF, **46(4)**, 143 (1987).

[6] J.L. Terry, E.S. Marmar, J.A. Snipes, D. Garnier, V.Yu. Sergeev, and TFTR Group, Rev. Sci. Instrum. **63**, 5191 (1992).

[7] S.M. Egorov, B.V. Kuteev, I.V. Miroshnikov, A.A. Mikhailenko, V.Yu. Sergeev, S.N. Ushakov, A.A. Bagdasarov, V.V. Chistyakov, D.Yu. Elizavetin, and N.L. Vasin, Nucl. Fusion **32**, 2025 (1992).

[8] R.K. Fisher, J.M. McChesney, A.M. Howald, P.B. Parks, D.M. Thomas, S.C. McCool, W.L. Rowan, Rev. Sci. Instrum. **61**, 3196 (1990).

[9] C. Andelfinger, E. Buchelt, P. Cierpka, H. Kollotzek, P.T. Lang, R.S. Lang, G. Prausner, F.X. Söldner, M. Ulrich, and G. Weber, Rev. Sci. Instrum. **64**, 983 (1993).

[10] A.E. Seigel, NATO Report AGARDograph-91, 1965.

[11] M.J. Gouge, S.K. Combs, P.W. Fisher, and S.L. Milora, Rev. Sci. Instrum. **60**, 570 (1989).

[12] S.M. Egorov, B.V. Kuteev, V.Yu. Sergeev, and A.V. Khekalo, Sov. Phys. Tech. Phys. **30(4)**, 408 (1985).

[13] L. Crocco, *Fundamentals of Gas Dynamics*, edited by H.W. Emmons (Princeton University Press, Princeton, 1958), chapter 2.